

The high-temperature behaviour of beryl melts and glasses

By R. P. MILLER, B.Sc., A.R.I.C. and R. A. MERCER

National Chemical Laboratory, Teddington, Middlesex

[Taken as read 3 June 1965]

Summary. The course of all crystalline structural changes undergone by the mineral beryl, its melt and glass, has been followed as a function of widely differing but accurately known thermal history. Non-equilibrium ordering processes have been characterized by new techniques in high-temperature microscopy.

The relative influence that beryllium and aluminium ions exert on the phase changes has been established by studies on synthetic melts and glasses representing hypothetical beryls of differing ratios of $\text{Be}^{2+}:\text{Al}^{3+}$ ions.

The dynamic changes between the oxide and orthosilicate structures into which the systems reconstitute include the formation of a metastable hybrid beryllium aluminium silicate, which is viewed as a beryllium-containing mullite. The crystallochemical changes have been interpreted in terms of a structural model of the melts and glasses that is shown to be consistent with the ordering effects predicted from the field strengths of the cations.

VERY little information is available on the formation and stability of beryl in the system $\text{BeO}-\text{Al}_2\text{O}_3-\text{SiO}_2$. Single crystal growth for gemstone or maser purposes is achieved at relatively low temperatures ($< 1000^\circ \text{C}$) either from hydrothermal or fluxed media. Until recently there were no reports of growth of beryl from a dry melt of its own or any other composition within the ternary system. A recent note,¹ however, reports that single crystals can be grown by flame-fusion methods and implies that beryl is a congruently melting compound. This view conflicts with that advanced by Van Valkenburg² who states that beryl melts incongruently at 1450°C into phenakite+liquid.

The fundamental processes that govern crystal growth must presumably be related to differences between the constitution of the melt and that of beryl, formation of which requires the stacking of cyclometasilicate $\text{Si}_6\text{O}_{18}^{12-}$ rings. The structural relationship between this crystal and its melt, besides being of fundamental interest, is important to the understanding and control of extraction procedures in beryllium metallurgy. Beryl is the principal raw material of this metal. The great chemical

¹ A. L. Gentile, D. M. Cripe, and F. H. Andres, *Amer. Min.*, 1963, vol. 48, p. 940.

² A. Van Valkenburg and C. E. Weir, *Bull. Geol. Soc. Amer.*, 1957, vol. 68, p. 1808.

stability of beryl has enforced the use of treatments at high temperature to break open the structure before being attacked by chemical reagents. One of the most direct of these methods is based upon a fusion-quench sequence in which the melt at 1700° C is quenched in water to a chemically reactive glass.¹ Although it has been recognized that the thermal history of the glass influences the efficiency of the subsequent acid attack the basic chemistry involved has been obscured by uncertainties surrounding the constitution of the melt and glass.

The problems involved in arriving at a structural model for melts and glasses are great since there is no technique capable of resolving all the questions about the nature of short-range order.

The complexities are underlined by the conflicting theories current on the nature of complex melts that can be quenched into the vitreous state. According to their overall compositions, silicate glasses can consist of microheterogeneous arrays of discrete ions in the form of rings, chains, sheets, or three-dimensional random networks.

It can be argued, and it is the approach adopted in this paper, that a detailed examination of the structures that crystallize from melts and glasses and of the associated kinetics affords strong presumptive evidence about the component species in the melt or glass.

This paper reports and discusses the results of a detailed examination of the thermal break-down of beryl and of the crystallization paths pursued by the melt and glass. The recently developed technique of thermal analysis by high-temperature microscopy² has formed the basis of a study in which all crystallization processes have been defined in terms of accurately known thermal history. Some preliminary observations were published earlier in a brief note.³ Similar studies have been made on synthetic melts and glasses corresponding to hypothetical beryls in which the ratio of $\text{Be}^{2+}:\text{Al}^{3+}$ has been varied. The implications of the results are discussed in connexion with the structure of the glasses.

Experimental techniques

High-temperature microscopy. The instrument used is an adaptation of that developed by Welch.⁴ Its basis is a thermocouple that is mounted on a microscope stage and can simultaneously function as a microfurnace and thermometer. Modifications to the circuitry have been made that allow continuous monitoring and recording of the cooling curves of melt droplets or the heating curves of glass

¹ C. B. Sawyer and B. R. F. Kjellgren, U.S. Pat. 1823864, 1931; 2018473, 1935; 2092621, 1937.

² R. A. Mercer and R. P. Miller, *Journ. Sci. Instr.*, 1963, vol. 40, p. 352.

³ R. A. Mercer and R. P. Miller, *Nature*, 1963, vol. 197, p. 683.

⁴ J. H. Welch, *Journ. Sci. Instr.*, 1954, vol. 31, p. 458.

beads between any two pre-selected temperatures. The technique has been described in detail elsewhere.¹

Differential thermal analysis (D.T.A.). The differential thermal analyser used was a commercial instrument manufactured by G. Netzsch. The thermograms were photographically recorded during heating rates of 10° C/min.

X-ray analysis. Powder photographs were taken in a Philips 11.46-cm camera. Copper radiation was used.

Infra-red measurements. The infra-red absorption spectra of the glasses were recorded by a Grubb Parsons GS3 instrument. Specimens were prepared by use of the pressed KCl disc technique.

Materials and reagents. Synthetic beryllium aluminium metasilicate glasses including that of ideal beryl composition were prepared by fusion of pure BeO, Al₂O₃, and SiO₂ in the appropriate ratios at 1700° C. The melts were quenched into water. The compositions of the products were checked by analysis. All the phase relationships studied by high-temperature microscopy were confirmed by multiple observations. Microanalytical checks were made on the microscopic specimens to ensure that no changes of composition occurred. Within the short time periods (up to 5 min) allowed for the microscopic droplets to equilibrate at 1700° C the composition remained unaltered. Over longer periods (> 15 min) there was serious loss of both SiO₂ and BeO at this temperature.

The natural beryls used in thermal breakdown studies ranged from a high-grade mineral (13.45 % BeO) of Brazilian origin to specimens of lower grade (about 10 % BeO) from Rhodesia. All behaved similarly during thermal breakdown.

Only the high-grade mineral was used for systematic studies concerned with melt and glass crystallization. There are indications, from other studies to be reported elsewhere, that variation in the alkali metal content of natural beryls affects the rate but not the nature of the various phase changes described. The thermal behaviour of synthetic melts and glasses of ideal beryl composition was identical with that of melts and glasses of the high-grade mineral.

The thermal decomposition of beryl

To establish whether there were any sub-solidus changes, natural beryls were equilibrated in conventional furnaces and on the hot-stage microscope at temperatures between 1100° and 1450° C. Within two days at 1100° C very weak lines of phenakite could be identified among the unchanged beryl spectrum. Up to 1420° C no increased degree of breakdown occurred but the weak lines of phenakite disappeared, giving way to equally weak lines of BeO and BeAl₂O₄. It was tentatively concluded that this breakdown was due to impurities, most likely alkali metal guest ions, which cause local weakening in the structure and premature collapse. The increased extent and rate of degradation of the lower-grade beryls under the same conditions was consistent with this conclusion. In such specimens the X-ray spectra of the breakdown products were relatively more intense although still very weak in relation to the dominant lines of beryl.

The melting process was observed under the hot-stage microscope.

¹ R. A. Mercer and R. P. Miller, *Journ. Sci. Instr.*, 1963, vol. 40, p. 352.

Sintering commenced at approximately 1300° C and small quantities of liquid were detected at 1460° C. A major degree of melting occurred at 1475° C but the collapse of the mineral was very sluggish. Clear melt was not obtained until the temperature exceeded 1600° C.

The melt between the temperatures 1475° and 1550° C was very viscous as judged by the lethargic movement both of the original beryl debris and the new crystalline species that grew and could be visually distinguished over this temperature range.

Between 1475° and 1600° C it was established by the microscopic technique that phenakite, chrysoberyl, and BeO had transient existence. It was concluded, in agreement with Van Valkenburg, that phenakite + liquid represents the structural state at the onset of melting. Increasing temperature brings about the progressive decomposition of phenakite into chrysoberyl + liquid, which in turn decomposes to BeO + liquid before the attainment of clear melt.

The occurrence of these peritectic relationships was confirmed over the temperature region 1450° to 1490° C by heat treatments of gram quantities of beryl in conventional furnaces. Although the sluggish rates of transformation did not permit precise determination of the transition temperatures, it was shown that between 1450° and 1475° C beryl degraded first into phenakite + liquid and then into chrysoberyl + liquid. These two crystalline phases co-existed for up to two days at 1475° C but further heating for 24 hours destroyed all the orthosilicate. Between 1475° and 1490° C the chrysoberyl gradually decomposed into BeO + liquid. After 6 hours at 1490° C BeO was the only crystalline phase.

The crystallization of beryl melts

Observations during slow cooling. The liquidus temperature and primary phase were established by observations on both synthetic and natural beryl melts. When droplets were slowly cooled (10° C/min) from 1700° C in the hot-stage microscope, hexagonal platelets of BeO grew and were judged to be in equilibrium with the melt at 1610° C. A typical formation is shown in fig. 1. The liquidus temperature was confirmed by more conventional quenching methods in which quantities of natural and synthetic melts were treated in an induction furnace assembly.

On further cooling, the crystals of BeO tended to precipitate as elongated needles and at 1450° C the specimen became generally opaque with the development of a cloudy microcrystalline growth of

chrysoberyl. Visual observation was thereafter made unrewarding by this characterless opacity. X-ray analysis revealed that within 4 hours at this temperature phenakite had appeared at the expense of BeO. At the end of this time only phenakite and chrysoberyl were present as crystalline phases.

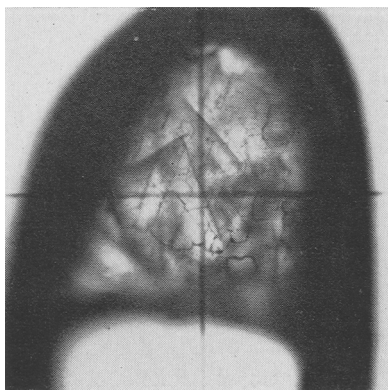


FIG. 1. Hexagonal plates of BeO grown from beryl melt at 1590° C.

Cooling to below 1450° C, however, did not result in the reconstitution of beryl as would be expected from a reversal of the breakdown sequences. All attempts to crystallize beryl from a melt or glass of its own composition have been unsuccessful.

Below 1400° C, BeO and chrysoberyl are joined by mullite and α (low)-cristobalite. The silica phase remains metastable but mullite subsequently decays. The associated disappearance of BeO and the growth of phenakite suggested that an independent reaction was occurring between the precipitated BeO and mullite. Separate studies with these two compounds have shown that a solid-state reaction does in fact occur to give chrysoberyl and phenakite. At all temperatures below 1450° C these two phases are compatible. At higher temperatures BeO and mullite make their appearance along with other metastable phases. (R. A. Mercer and R. P. Miller, *Nature*, 1964, vol. 202, p. 581).

Table I summarizes the phases initially appearing at successively lower temperatures when the melts are cooled at 10° C/min. The course of any secondary reactions occurring during relatively short retention times are also shown. These secondary changes are dealt with more fully in the studies on glass devitrification.

In addition to the phases listed in table I other weak lines appeared.

These were later identified as belonging to the larger cell modification of a new beryllium aluminium silicate phase. The X-ray powder data on this phase, the conditions that govern its formation, and its stability within this system are detailed later.

The thermal analysis of beryl melts during rapid cooling. The cooling curves of microscopic droplets of melt, air-quenched from 1700° C to temperatures between 1500° and 20° C are shown in fig. 2, *a-j*. The phases responsible for the arrests are listed in table II along with those

TABLE I. Phase generation on cooling beryl melts at 10° C per minute from 1700° C.

Final temperature, ° C	Retention time at final temperature minutes	Phases identified by X-ray analysis
1610	quenched immediately	BeO
1450	quenched immediately	BeO, BeAl ₂ O ₄
1450	240	Be ₂ SiO ₄ , BeAl ₂ O ₄
1400	quenched immediately	BeO, BeAl ₂ O ₄ , mullite
1400	30	BeO, BeAl ₂ O ₄ , mullite, α (low)-cristobalite
1400	240	BeO, BeAl ₂ O ₄ , α (low)-cristobalite
1350 and all lower temperatures	quenched immediately or after 30 min	BeO, BeAl ₂ O ₄ , mullite, α (low)-cristobalite

phases that subsequently grow within 1 hour on holding at the lower limiting temperature. The cooling rates measured to the arrest temperature are also given.

When the sample was cooled to 1500° C at 80° C/sec the cooling curve was smooth, but within seconds of the attainment of this temperature, small needles of BeO grew radially from centres randomly distributed throughout the melt. These grew rapidly and converted the specimen to complete opacity. On quenching to 1400° C, the cooling rate was increased to 150° C/sec; at this cooling rate the temperature at which BeO crystallized was depressed to 1430° C. The cooling curve arrest at this temperature can be regarded as the pseudo-liquidus associated with that particular rate of undercooling. Swift precipitation of the microcrystalline oxide can be visually observed to coincide with the exothermic effect.

Chrysoberyl, mullite, and α (low)-cristobalite grew and were present after 1 hour. When the lower limiting temperature was pre-set to 1300° or 1200° C the rate of quenching was further increased.

At a cooling rate of 200° C/sec, BeO and mullite simultaneously

precipitated at the pseudo-eutectic temperature of 1380° C. This temperature was depressed to 1320° C when the rate of cooling was increased to 250° C/sec. If the cooling rate imposed on the melt was increased to 350° C/sec by air-quenching to 1100° C, the BeO/mullite eutectic was further depressed to 1310° C, but an additional consecutive exotherm

TABLE II. Thermal analysis of beryl melts

Temperature range over which the specimen was quenched, ° C	Temperature of arrest, ° C	Rate of cooling to arrest, ° C/sec	Phases generated during quenching	Phases identified after retention of 1 hour	
1700-1500	...	No arrest	80*	BeO*	BeO, BeAl ₂ O ₄
1700-1400	...	1430	150	BeO	BeO, BeAl ₂ O ₄ , mullite, α (low) cristobalite
1700-1300	...	1380	200	BeO, mullite	BeO, BeAl ₂ O ₄ , mullite, α (low)- cristobalite
1700-1200	...	1320	250	BeO, mullite	BeO, BeAl ₂ O ₄ , mullite, α (low)- cristobalite
1700-1100	...	{ 1310 1220	350†	{ BeO mullite hybrid	{ BeO, mullite, hybrid, α (low)- cristobalite
1700-1000	...	1240	400	hybrid	BeO, mullite, hybrid
1700-900	...	1220	450	hybrid	BeO, hybrid
1700-800	...	1180	500	hybrid	hybrid
1700-20	...	1080	500	hybrid	hybrid
1700-20	...	No arrest	750‡	none	none

* BeO appeared within seconds of the melt attaining 1500° C. The rate of cooling recorded is that between 1700° and 1500° C.

† Rate of cooling to the first arrest.

‡ A smaller quantity of melt was used. The rate of cooling shown was that between 1700° and 1100° C.

appeared, which arrested the curve at 1220° C. Visual observation on specimens cooled under these conditions showed a further sudden increase in optical density immediately following the general opalescence arising from the explosive growth of BeO and mullite. In addition to the X-ray powder spectrum of these two species, other lines of the new beryllium aluminium phase mentioned earlier appeared on the photographs. That the crystallization of this phase caused the arrest at 1220° C was proved by water-quenching a melt droplet showing these double heat effects immediately after the first arrest. Only BeO and mullite were present. Further, when the rate of cooling was increased to

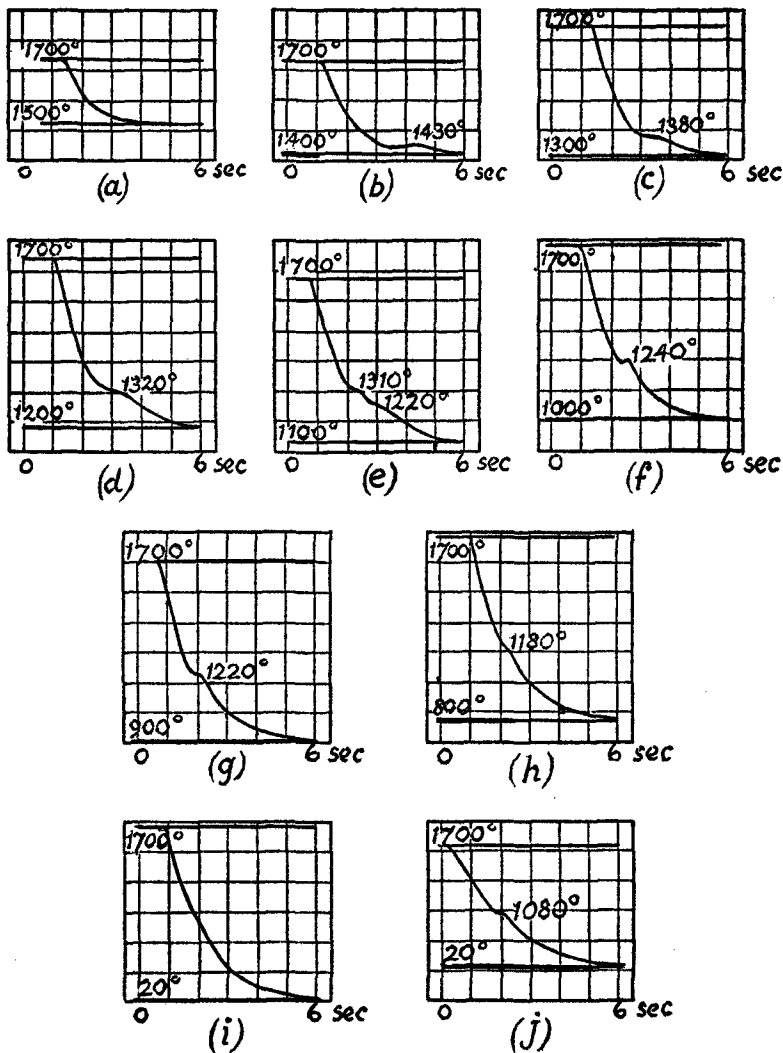
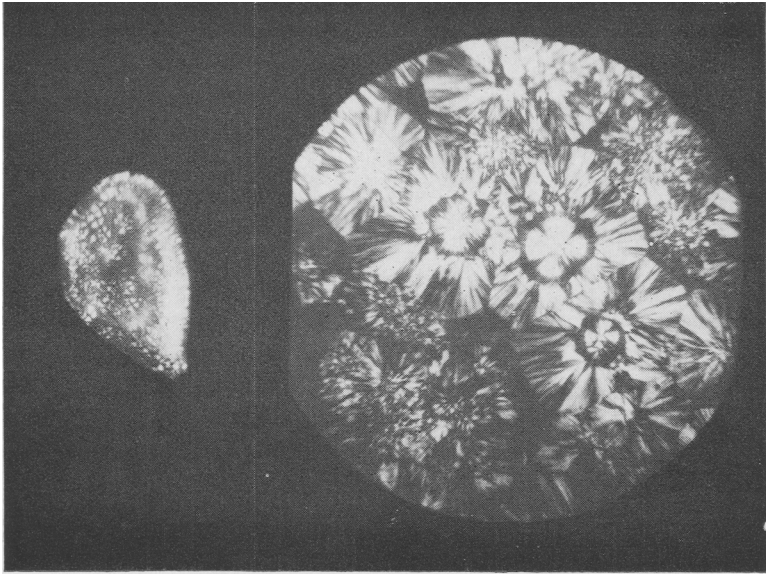


FIG. 2. Cooling curves for beryl melts quenched in air from 1700° C to various temperatures.

400° C/sec the precipitation of BeO and mullite no longer occurred and only the one arrest at 1220° C appeared on the cooling curve; the only crystalline phase present was the hybrid silicate. The unit-cell size of the phase produced in this manner was smaller than that thrown out of

the beryllium-deficient melts, i.e. beryl melts partially devitrified into BeO, or the synthetic melts described later. Under the polarizing microscope, the phase can be seen to be dispersed as spherulites in a glassy matrix (fig. 3).



FIGS. 3 and 4: FIG. 3 (left). Spherulites of beryllium aluminium hybrid silicate precipitated by chilling beryl melts at 400°C per second. FIG. 4 (right). Microstructure of beryl glass devitrified into BeO, mullite, and beryllium aluminium hybrid silicate.

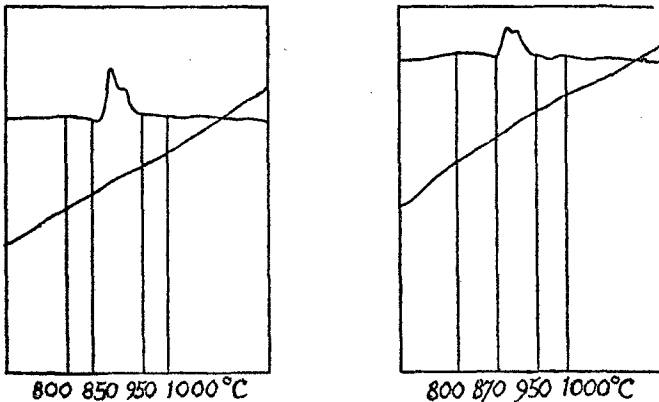
Progressive lowering of the temperature to which the melts were air-quenched caused a corresponding depression of the liquidus temperature of this 'quench' phase. At rates of chilling above $750^{\circ}\text{C}/\text{sec}$, X-ray-amorphous glasses were always produced. The only diffraction effect in these was a broad diffuse halo straddling the position of the very intense 101 reflection of α (low)-crystalite.

Although the detailed correlation between cooling-rate variation and primary-phase generation was possible only by the technique of high-temperature microscopy, a sufficient variation in the quenching rates of 100-g batches of beryl melts could be attained to reproduce the crystallochemical changes characterized microscopically. Thus on streaming a melt at 1700°C into water, the larger beads of glass, whose

centres had cooled more slowly than the surface, could be differentiated by their blue translucence. This feature was shown to be due to spherulites of the hybrid phase. When a similar melt was quenched by being poured on to a metal plate, the product was generally opalescent due to the crystallization of BeO, mullite, and the hybrid. The spherulitic microstructure of such a product is shown by the polished section (fig. 4).

The devitrification of beryl glasses

The primary ordering processes in beryl glasses depend upon the rate of heating. X-ray-amorphous glasses leisurely heated to 1200° C (10° C/min) in the differential thermal analyser showed an exothermic reaction be-



FIGS. 5 and 6: Differential thermal curves. FIG. 5 (left): Curve for beryl glass derived from pure oxides. FIG. 6 (right): Curve for pure oxide beryl glass partially crystallized into a modified phenacite.

tween 850° and 950° C. The peak profile was saddled (fig. 5), suggesting that at least two phases were responsible, the crystallization temperatures of which were too close for differentiation; X-ray analysis showed BeO, mullite, chrysoberyl, and α (low)-cristobalite had all appeared; in a separate experiment in which the specimen was removed immediately after the exotherms, only BeO and mullite were present. Thermograms of glasses partially devitrified into the beryllium aluminium silicate hybrid (fig. 6) were similar to those of the amorphous glasses; the product, after differential thermal analysis, contained BeO, mullite, and α (low)-cristobalite in addition to the original hybrid. No heat effect was shown during differential thermal analysis of glassy products

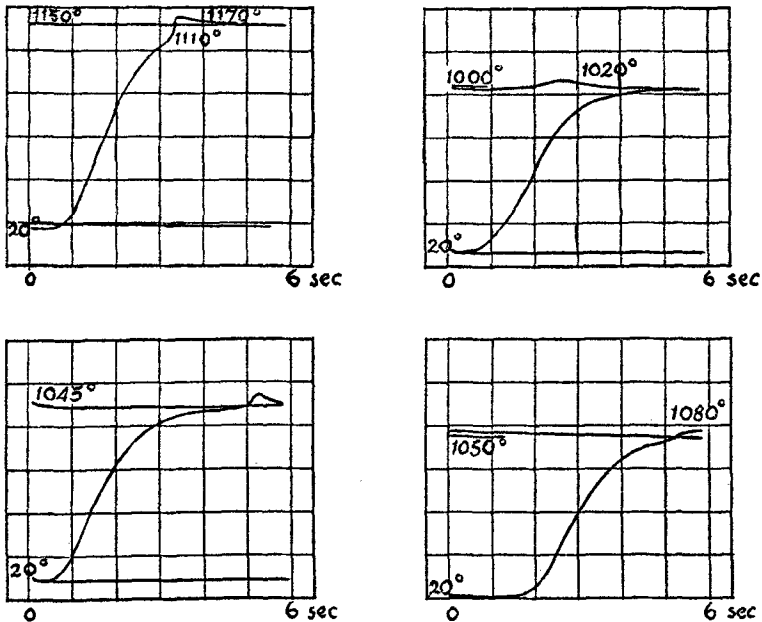
previously devitrified into BeO, mullite, and the hybrid; X-ray analysis afterwards, however, showed that α (low)-cristobalite had crystallized during the heating.

When X-ray-amorphous glasses were shock-heated in the hot-stage microscope, only the smaller-cell hybrid phase spontaneously precipitated. The heating curves of samples shock-heated from room temperature to temperatures between 1000° and 1500° C all showed a discontinuity coinciding with the precipitation of spherulites of this hybrid phase; the precipitation temperature depended upon the rate of heating and varied between 1000° and 1170° C. The effect recorded on heating to 1150° C is shown in fig. 7; a heat pulse between 1110° and 1170° C interrupted the otherwise smooth heating curve; the heating rate to the beginning of this effect was 500° C/sec. Induction periods preceded the generation of the hybrid phase when glasses were shock-heated to temperatures between 1000° and 1050° C. The measurable time periods that elapsed before the exothermic effect was recorded depended upon the upper limiting temperature chosen within this range. Examples are shown in figs. 8 and 9.

A clear demonstration that the generation of the hybrid phase only arises if insufficient time is allowed for ionic rearrangements to occur in the glass at lower temperatures was given by heating an X-ray-amorphous glass on the microscope for 1 hour at 850° C. Such treatment does not induce any crystallization. Water-quenching from this temperature followed by shock-heating from room temperature to 1050° C induces a comparable heat effect (fig. 10) to that shown by an unconditioned glass. The crystal phases responsible, however, were BeO and mullite, and not the hybrid.

Partially devitrified glassy products, whether containing BeO and mullite or the hybrid, reached the same final crystalline state on prolonged heating; the times taken to effect these changes were, however, different. The changes were examined during conventional furnace and microfurnace equilibrations of specimens devitrified into the states described. In all glasses, heating to 1400° C produced chrysoberyl, phenakite, and α (low)-cristobalite, after the formation of which there was no tendency for further change. Above 1400° C the silica phase rapidly disappeared and the peritectic sequence described earlier ($\text{Be}_2\text{SiO}_4 + \text{liq.} \rightarrow \text{BeAl}_2\text{O}_4 + \text{liq.} \rightarrow \text{BeO} + \text{liq.}$) occurred. Below this temperature it was obvious that the rate of interaction of BeO and mullite to give chrysoberyl and phenakite was much slower than the disruption of the hybrid to give the same products. For example at 1150° C a poorly

crystallized hybrid (diffuse X-ray spectrum) produced by quenching a melt at 1700°C , at a rate just below the threshold rate ($750^{\circ}\text{C}/\text{sec}$) above which X-ray-amorphous glasses are formed, had decayed within



FIGS. 7-10: Curves showing devitrification on rapid heating. FIG. 7 (top left): Exothermic effect accompanying generation of beryllium aluminium hybrid silicate; heating rate to 1110°C , $500^{\circ}\text{C}/\text{sec}$. FIG. 8 (top right): Beryl glass shock heated to 1000°C ; exotherm occurs 3 seconds after attaining 1000°C . The phase generated was beryllium aluminium hybrid silicate. FIG. 9 (bottom left): Beryl glass shock heated to 1045°C ; exotherm occurs immediately. The phase generated was beryllium aluminium hybrid silicate. FIG. 10 (bottom right): Pre-heated beryl glass shock heated to 1050°C ; the broadened exotherm signals precipitation of BeO and mullite.

30 minutes. Reaction was incomplete, after 24 hours at this temperature, in a glassy product containing BeO and mullite.

The rate at which the hybrid decayed was measured approximately at differing temperatures by following the relative intensity changes between the 100 reflection of this phase and the 110 reflection of the phenakite produced; these two lines form a close doublet on the photographs. Systematic kinetic studies were not attempted since it was clear that the degree of crystallinity of the hybrid influenced the rate at which it

decomposed. In contrast to the rapid breakdown noted above of the poorly crystallized hybrid, well-developed spherulites prepared by air-quenching beryl melts in the microscope at $400^{\circ}\text{C}/\text{sec}$ were incompletely transformed to phenakite and chrysoberyl after 90 minutes at 1300°C . The transition was complete at this temperature within 2 hours; at 1400°C , reaction was complete within 10 minutes. This dependence of decay rate on crystallite size shows that the thermal decomposition is not of the first order. The mechanism presumably involves diffusion of ions out of the crystals with product formation at the boundaries. The interesting observation was made that during the transformation the unit cell enlarged. Simultaneously with the first appearance of the lines of chrysoberyl and phenakite on the photographs an increase in the interplanar spacings of the hybrid occurs, allowing confident indexing on the larger cell that characterizes the hybrid precipitated from aluminium-rich melts. This behaviour was common to many observations.

Infra-red absorption by beryl glasses

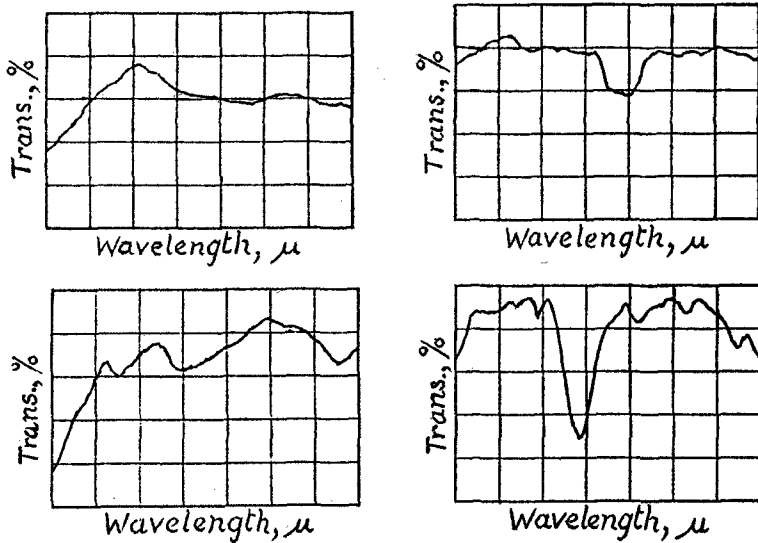
X-ray-amorphous beryl glasses possess two broad absorption bands with maxima at 1080 cm^{-1} ($9.25\ \mu$) and 800 cm^{-1} ($12.5\ \mu$) (fig. 11). This spectrum is very similar to that of fused silica, which is a broadened version of the crystalline cristobalite spectrum. The glassy product containing phenakite, chrysoberyl, and α (low)-cristobalite (fig. 12) shows peaks characteristic of the individual crystalline compounds (figs. 13 and 14). The resolution, however, was too poor to afford any data on the hybrid phase. A glass in which spherulites of this phase were present showed no difference in infra-red absorption from that of the amorphous glass.

The relative influence of Be^{2+} and Al^{3+} ions on phase generation in melts and glasses of metasilicate composition

The compositions of the systems examined lay on the join between the binary points $\text{BeO}\cdot\text{SiO}_2$ and $\text{Al}_2\text{O}_3\cdot 3\text{SiO}_2$. Phase generation from the melts and glasses was studied under similar conditions to those described for beryl.

Crystallization from the melts. The liquidus temperature and primary phases at the compositions chosen are shown in table III. The primary phase boundary between BeO and mullite is crossed at the higher aluminium ratios. In the high-beryllium melt, accuracy in the determination of the liquidus temperature was limited by the rapid composition

change suffered at temperatures above 1700° C. In the more aluminous systems there was a marked tendency to undercooling. The crystallization of mullite needles was frequently delayed to 100–200° C below the temperature finally judged to be the liquidus. Their dissolution, once



FIGS. 11–14: Infra-red transmission spectra. FIG. 11 (top left): Amorphous beryl glass. FIG. 12 (top right): Beryl glass crystallized into phenacite chrysoberyl, and α (low) cristobalite. FIG. 13 (bottom left): chrysoberyl. FIG. 14 (bottom right): Natural phenacite.

TABLE III. Primary phases and liquidus temperatures at selected beryllium aluminum metasilicate compositions

Systems	Primary phase	Liquidus temp. ° C
$4\text{BeO} \cdot \frac{2}{3}\text{Al}_2\text{O}_3 \cdot 6\text{SiO}_2$	BeO	1675 ± 20
$3\text{BeO} \cdot \text{Al}_2\text{O}_3 \cdot 6\text{SiO}_2$	BeO	1610 ± 5
$2\text{BeO} \cdot 1\frac{1}{2}\text{Al}_2\text{O}_3 \cdot 6\text{SiO}_2$	mullite	1640 ± 20
$\text{BeO} \cdot 1\frac{2}{3}\text{Al}_2\text{O}_3 \cdot 6\text{SiO}_2$	mullite	1730 ± 20
$\frac{1}{2}\text{BeO} \cdot 1\frac{5}{6}\text{Al}_2\text{O}_3 \cdot 6\text{SiO}_2$	mullite	1750 ± 20

formed, was very sluggish. Their typical needle morphology, when crystallizing from these melts, is shown in fig. 15.

The initial phases spontaneously generated from the melts during thermal analysis by high-temperature microscopy are recorded in table IV. The relationship is shown between the emergence temperature and the cooling rate imposed. As the relative concentration of Be^{2+} ions

was lowered, the cooling rate necessary for glass formation progressively decreased and the crystal structures generated changed. It was found to be impossible to air-quench the high-beryllium melt in the microscope

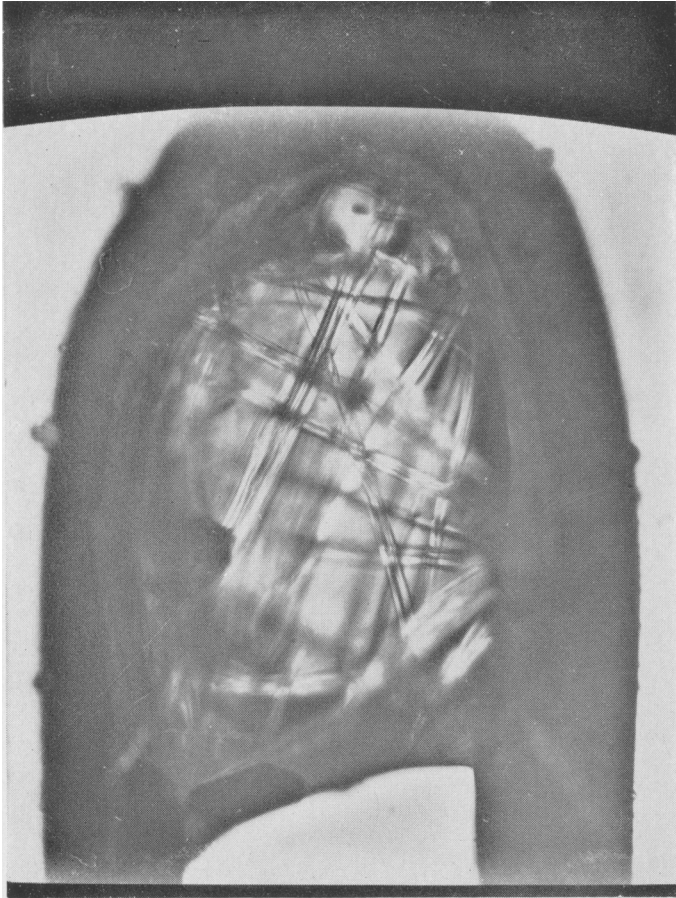


Fig. 15. Mullite needles growing at 1700° C from a melt of composition $\text{BeO} \cdot 1\frac{2}{3}\text{Al}_2\text{O}_3 \cdot 6\text{SiO}_2$.

to a glass, the limiting rate of chilling by this means being about 1100° C/sec; either BeO and mullite or the hybrid phase (smaller unit cell) precipitated according to the cooling rate; glass formation was readily effected by water-quenching in the microscope (*c.* 10 000° C/sec). At this composition there was some visible evidence suggestive of immiscibility;

TABLE IV. Thermal analyses of beryllium aluminium metasilicate melts

System composition	Temperature range over which melts were quenched, ° C	Arrest temperature ° C	Rate of cooling to arrest, ° C/sec	Phase(s) responsible for arrest
4BeO. $\frac{2}{3}$ Al ₂ O ₃ . 6SiO ₂	1800-1500	—	200 (to 1500° C)	No phase spontaneously generates. BeO grows within seconds at 1500° C
	1800-1400 } 1800-900 }	1450 } 1375 }	200 } 655 }	BeO mullite
	1800-20	1360	1100	hybrid*
2BeO. 1 $\frac{1}{3}$ Al ₂ O ₃ . 6SiO ₂	1700-1300	—	200 (to 1300° C)	No phase spontaneously generates
	1700-1200 } 1700-1100 }	1220 } 1185 }	240 } 390 }	hybrid†
	1700-1050	—	430 (to 1185° C)	No phase spontaneously generates
	1800-1300 } 1800-1250 }	1275 } 1215 }	170 (to 1300° C) 180 } 280 }	No phase spontaneously generates
BeO. 1 $\frac{2}{3}$ Al ₂ O ₃ . 6SiO ₂	1800-1150 } 1800-1100 }	—	360 (to 1215° C)	No phase spontaneously generates
	1800-1300 } 1800-1200 }	—	230 (to 1300° C) 295 }	No phase spontaneously generates
1 $\frac{1}{3}$ BeO. 1 $\frac{5}{6}$ Al ₂ O ₃ . 6SiO ₂	1800-1000	—	560 (to 1240° C)	No phase spontaneously generates

* Smaller unit cell. † Larger unit cell.

quenching of the melt from 1800° C to temperatures between 1500° and 1650° C caused precipitation of BeO as fern-like sprays which appeared to grow within globular boundaries separated from clear melt.

The only phase spontaneously generated from the melt of composition $2\text{BeO} \cdot 1\frac{1}{3}\text{Al}_2\text{O}_3 \cdot 6\text{SiO}_2$ at cooling rates below 400° C/sec was the hybrid phase with the larger unit cell. Swifter quenching rates resulted in glass transformation.

The remaining melts of higher alumina content precipitated only mullite within the narrower cooling rate limits shown in table IV.

TABLE V. Structural changes in beryllium aluminium metasilicate glasses during D.T.A. to 1200° C

Composition	Temperature of exotherm, ° C	Phases present after D.T.A. †
$4\text{BeO} \cdot \frac{2}{3}\text{Al}_2\text{O}_3 \cdot 6\text{SiO}_2$	No heat effect*	BeO,* mullite,* α (low)-cristobalite
$2\text{BeO} \cdot 1\frac{1}{3}\text{Al}_2\text{O}_3 \cdot 6\text{SiO}_2$	930-980	mullite, hybrid, † α (low)-cristobalite
$\text{BeO} \cdot 1\frac{2}{3}\text{Al}_2\text{O}_3 \cdot 6\text{SiO}_2$	925-1000	mullite, Be_2SiO_4 , α (low)-cristobalite
$\frac{1}{2}\text{BeO} \cdot 1\frac{5}{6}\text{Al}_2\text{O}_3 \cdot 6\text{SiO}_2$	950-1000	mullite

* BeO and mullite were present before D.T.A.

† Larger unit cell.

Devitrification of the glasses. Structural changes occurring within these glasses were examined during differential thermal analysis, microscopic thermal analysis, and equilibrations at various temperatures in conventional furnaces. The results are summarized in tables V and VI.

All the glasses with higher aluminium contents than that of beryl exhibited one exothermic effect during differential thermal analysis, which was shown to be due to crystallization of mullite. The other phases shown in table V grew during the further heating. An X-ray-amorphous glass of composition $4\text{BeO} \cdot \frac{2}{3}\text{Al}_2\text{O}_3 \cdot 6\text{SiO}_2$ could not be obtained on the macro scale. The product of water-quenching a 1-g melt of this composition contained BeO and mullite. No heat effect was shown during D.T.A. but this product resembled beryl glasses in a similar partially crystalline condition in that α (low)-cristobalite crystallized during the analysis.

The phases spontaneously generated when the glasses were shock-heated in the microscope to various temperatures are shown in table VI. The secondary transformations occurring during retention times, ranging from 1 hour to 5 days, are also included.

TABLE VI. Crystallization of beryllium aluminum metasilicate glasses (phases produced in the systems)

Temp., ° C	Retention time at temp., hours	4BeO. 3Al ₂ O ₃ . 6SiO ₂		2BeO. 1 1/3 Al ₂ O ₃ . 6SiO ₂		BeO. 1 1/2 Al ₂ O ₃ . 6SiO ₂		1/2 BeO. 1 1/4 Al ₂ O ₃ . 6SiO ₂	
		Temp., ° C	Ret. time, hours	Phases	Phases	Phases	Phases	Phases	Phases
1000	BeO	hybrid†	mullite	mullite	mullite	mullite
1100	0	BeO, mullite	hybrid†	mullite	mullite	mullite	mullite
"	1	BeO, mullite	hybrid, †	mullite	mullite	mullite	mullite
"	24	BeO, mullite, α (low)-cristobalite	Be ₂ SiO ₄ , mullite, α (low)-cristobalite	mullite, Be ₂ SiO ₄	mullite	mullite	mullite
"	120	beryl, Be ₂ SiO ₄ , BeAl ₂ O ₄ , α (low)-cristobalite	beryl, Be ₂ SiO ₄ , mullite, α (low)-cristobalite	—	—	—	—
1200	0	BeO, mullite	hybrid†	mullite	mullite	mullite	mullite
"	1	BeO, mullite	hybrid, †	mullite, α (low)-cristobalite	mullite, α (low)-cristobalite	mullite	mullite
"	24-72	beryl, Be ₂ SiO ₄ , BeAl ₂ O ₄ , α (low)-cristobalite	beryl, Be ₂ SiO ₄ , mullite, α (low)-cristobalite	mullite, α (low)-cristobalite	mullite, α (low)-cristobalite	mullite	mullite
1300	0	BeO, mullite	hybrid†	mullite	mullite	mullite, α (low)-cristobalite	mullite, α (low)-cristobalite
"	1	Be ₂ SiO ₄ , mullite, α (low)-cristobalite	hybrid, † Be ₂ SiO ₄ , BeAl ₂ O ₄ , mullite, α (low)-cristobalite	mullite, Be ₂ SiO ₄ , α (low)-cristobalite	mullite, Be ₂ SiO ₄ , α (low)-cristobalite	mullite, α (low)-cristobalite	mullite, α (low)-cristobalite
"	24	beryl, Be ₂ SiO ₄ , BeAl ₂ O ₄ , α (low)-cristobalite	beryl, Be ₂ SiO ₄ , BeAl ₂ O ₄ , mullite, α (low)-cristobalite	beryl, mullite, α (low)-cristobalite	beryl, mullite, α (low)-cristobalite	mullite, α (low)-cristobalite	mullite, α (low)-cristobalite
1400	0	hybrid, † Be ₂ SiO ₄ , mullite, α (low)-cristobalite	hybrid†	mullite	mullite	mullite, α (low)-cristobalite	mullite, α (low)-cristobalite
"	1	Be ₂ SiO ₄ , BeAl ₂ O ₄	hybrid, † Be ₂ SiO ₄ , mullite, α (low)-cristobalite	mullite, Be ₂ SiO ₄ , α (low)-cristobalite	mullite, Be ₂ SiO ₄ , α (low)-cristobalite	mullite, α (low)-cristobalite	mullite, α (low)-cristobalite
"	24	Be ₂ SiO ₄ , BeAl ₂ O ₄	beryl, Be ₂ SiO ₄ , BeAl ₂ O ₄ , α (low)-cristobalite	—	—	mullite, α (low)-cristobalite	mullite, α (low)-cristobalite
1475	24	Be ₂ SiO ₄	BeAl ₂ O ₄	mullite	mullite	mullite	mullite
1500	1	BeO, BeAl ₂ O ₄ , Be ₂ SiO ₄	hybrid, † mullite, α (low)-cristobalite	mullite, α (low)-cristobalite	mullite, α (low)-cristobalite	mullite	mullite

* Zero in this column signifies immediate quenching. † Larger unit cell. ‡ Smaller unit cell.

The most striking consequence of altering the $\text{Be}^{2+}:\text{Al}^{3+}$ ratio from that of ideal beryl ($3\text{Be}^{2+}:2\text{Al}^{3+}$) is the ultimate appearance of beryl from all the systems except the most aluminous, from which no crystalline beryllium phase was produced.

The stability of the hybrid phase was considerably enhanced in the system $2\text{BeO}\cdot 1\frac{1}{3}\text{Al}_2\text{O}_3\cdot 6\text{SiO}_2$ and, within this system, was always contained in the larger unit cell. In general terms it can be seen that a decrease in the Be^{2+} ion concentration relative to Al^{3+} tended to eliminate the formation, as primary phases, of the oxide structures BeO and BeAl_2O_4 and to increase the early predominance of orthosilicates through the sequence Be_2SiO_4 , Be/Al hybrid, and mullite.

X-ray-powder data and unit cell dimensions of the hybrid beryllium aluminium silicate phases

It will be recalled that the smaller cell structure (hybrid 1 in table VII) appeared both as a quench phase from clear beryl melts and as a result of the rapid heating of X-ray-amorphous beryl glasses. It also appeared, less readily, from the clear melts and glasses of composition $4\text{BeO}\cdot 2\frac{2}{3}\text{Al}_2\text{O}_3\cdot 6\text{SiO}_2$ under similar conditions.

The larger cell characterizes the structure (hybrid 2) that precipitated as a quench phase from beryl melts partially crystallized into BeO and from melts and glasses of composition $2\text{BeO}\cdot 1\frac{1}{3}\text{Al}_2\text{O}_3\cdot 6\text{SiO}_2$; it also appeared as an intermediate structure during the course of the thermal decomposition of hybrid 1.

Table VII lists the interplanar spacings of these two structures and includes the characteristic spectrum of phenakite. It became evident that the correspondence of all the lines of the hybrid with some of those of phenakite is such that expanded phenakite cells are completely consistent with the data. The parameters of such cells are tabulated. The possibility that these compounds were expanded derivatives of phenakite had therefore to be considered. Such an expansion is readily visualized as arising from Al^{3+} ion substitution, 2Al^{3+} simultaneously occupying a Be^{2+} and Si^{4+} site in the lattice. It can be seen, however, that all the reflections from natural phenakite for which l is neither 0 nor divisible by 3 have no counterpart in those that characterize the new phases if indexed on the phenakite-type cell. These systematic absences are highly suggestive of a change of symmetry in which event the true unit cell would be smaller. In fact the hybrid pattern can be satisfactorily re-indexed (see table IX) on a smaller hexagonal cell. However, the possibility that these absences may have

TABLE VII. Interplanar spacing values of the new beryllium aluminium silicates and of phenakite.

Normal phenakite			Hybrid 1		Hybrid 2	
Hexagonal cell	a 12.47 Å, c 8.25 Å		Indexed on hexagonal cell	a 12.78 Å, c 8.49 Å	Indexed on hexagonal cell	a 12.90 Å, c 8.64 Å
	hkl	d	d	I	d	I
11 $\bar{2}$ 0	6.24 Å	40	6.41 Å	m	6.47 Å	m
02 $\bar{2}$ 1	4.52	3	—	—	—	—
01 $\bar{1}$ 2	3.86	25	—	—	—	—
21 $\bar{3}$ 1	3.66	80	—	—	—	—
30 $\bar{3}$ 0	3.601	30	3.69	m	3.73	m
2022	3.279	3	—	—	—	—
22 $\bar{4}$ 0	3.119	100	3.19	ms	3.23	ms
12 $\bar{3}$ 2	2.903	17	—	—	—	—
13 $\bar{4}$ 1	2.817	13	—	—	—	—
11 $\bar{2}$ 3	2.518	75	2.58	ms	2.62	ms
41 $\bar{5}$ 0	2.358	70	2.42	m	2.44	m
04 $\bar{4}$ 2	2.262	5	—	—	—	—
30 $\bar{3}$ 3	2.187	60	2.24	m	2.27	m
3360	2.079	50	2.13	m	2.15	mw
10 $\bar{1}$ 4	2.026	3	—	—	—	—
2461	1.982	9	—	—	—	—
50 $\bar{5}$ 2	1.914	9	—	—	—	—
21 $\bar{3}$ 4	1.842	3	—	—	—	—
42 $\bar{6}$ 2	1.829	3	—	—	—	—
6060	1.798	5	—	—	—	—
41 $\bar{5}$ 3	1.790	15	1.84	w	1.86	vw
1562	1.755	3	—	—	—	—
43 $\bar{7}$ 1	1.735	7	—	—	—	—
5270	1.730	11	1.77	w	1.79	vw
3363	1.658	17	1.70	w	1.72	mw
4044	1.639	3	—	—	—	—
1671	1.615	3	—	—	—	—
3254	1.585	1	—	—	—	—
6172	1.530	7	—	—	—	—
6063	1.506	25	1.54	mw	1.56	mw
0554	1.492	1	—	—	—	—
6281	1.473	7	—	—	—	—
3145 } 0772 }	1.446	1	—	—	—	—
7180	1.431	25	1.46	w	1.48	w
5164	1.413	1	—	—	—	—
0445 } 2682 }	1.408	1	—	—	—	—
0006	1.376	9	1.41	w	1.43	w
2355	1.374	6	—	—	—	—
6390	1.361	5	—	—	—	—
			1.32	mw	1.30	m

arisen through destructive interference of the diffracted rays due to the substitution of Al^{3+} ions in selected sites could not be excluded. Since the conception of the nature of these phases depends upon a confident selection between these two alternatives, structure factor calculations were undertaken to see how various modes of substitution of Al^{3+} ions in normal phenakite would affect the intensity of the reflections in question.

Although there would be only one plausible mode of substitution, namely simultaneous exchange of Al^{3+} for both Be^{2+} and Si^{4+} , calculations were also made on the less likely interchange of Al^{3+} in only the Be^{2+} positions, charge balance being preserved by Si^{4+} absences. Since the aim of the calculations was to establish whether such an ion interchange could effectively destroy the reflections concerned, an extreme degree of replacement was assumed. Failure, then, to show that the intensity would become vanishingly small would mean that any lesser and more likely degree of substitution must be ruled out. Accordingly, the two possible modes suggested above were assumed to occur to such an extent that in the first alternative (simultaneous substitution) 75 % of the Si^{4+} positions would be occupied. The hypothetical composition would then be $\text{Be}_5\text{Al}_3\text{SiAl}_3\text{O}_{16}$. For the second alternative ($\text{Be}^{2+}/\text{Al}^{3+}$ interchange) the calculations were based on a 50 % replacement of Be^{2+} ions in which case the hypothetical composition would become $\text{Be}_4\text{Al}_4\text{Si}_3\text{O}_{16}$, with 25 % of the Si^{4+} positions untenanted.

It can be seen from table VII that the more strongly reflecting forward reflections from phenakite that have no detectable counterpart in the new structures are the $01\bar{1}2$, $21\bar{3}1$, $12\bar{3}2$, $13\bar{4}1$, $24\bar{6}1$, and $50\bar{5}2$. These were the reflections, therefore, that were considered in the structure-factor calculations.

Table VIII compares the calculated and observed intensities of these reflections for the normal mineral and the calculated intensities that would hold if the mineral were substituted in the manner discussed. It is clear that an Al^{3+} ion substitution in the phenakite structure, in such a way that the basic oxygen-ion framework is maintained, is not consistent with the data. A powder photograph of normal phenakite mixed with amorphous beryl glass in such proportion that the intensities of its strong lines were comparable with those of the new phases after 24 hours exposure (standard throughout all the work) clearly showed the lines of 3–5 % relative intensity.

Similar structure-factor calculations on the effect of the substitution on the most intense $22\bar{4}0$ reflection showed that no marked change in

TABLE VIII. Calculated intensities of selected reflections of phenakite and the effect of substitution of Al^{3+} ions

hkl	Natural Be_2SiO_4		Hybrids 1 and 2		
	I (calc.)	I (obs.)	I (calc.)		I (obs.)
			(A)	(B)	
01 $\bar{1}$ 2	28	25	10	0.1	0
21 $\bar{3}$ 1	80	80	43	13	0
12 $\bar{3}$ 2	11	17	4	0.4	0
1341	7	13	2	0.4	0
24 $\bar{6}$ 1	4	9	2.5	1.0	0
50 $\bar{5}$ 2	4	9	1.0	0	0

(A) Intensities calculated on the basis of simultaneous Al^{3+} ion substitution for Be^{2+} and Si^{4+} .

(B) Intensities calculated on the basis of $\text{Al}^{3+}/\text{Be}^{2+}$ interchange.

TABLE IX. Unit-cell dimensions and indexed diffractions for the new beryllium aluminium silicates. Hexagonal cells

hkl	d^*	Hybrid 1 a 7.38 Å, c 2.82 Å		d^*	Hybrid 2 a 7.46 Å, c 2.87 Å	
		$\sin^2 \theta$			$\sin^2 \theta$	
		obs.	calc.		obs.	calc.
10 $\bar{1}$ 0	6.41	0.0144	0.0146	6.47	0.0142	0.0142
11 $\bar{2}$ 0	3.69	0.0436	0.0437	3.73	0.0426	0.0427
20 $\bar{2}$ 0	3.19	0.0583	0.0583	3.23	0.0570	0.0569
10 $\bar{1}$ 1	2.58	0.0889	0.0894	2.62	0.0864	0.0866
21 $\bar{3}$ 0	2.42	0.1017	0.1020	2.44	0.0996	0.0996
11 $\bar{2}$ 1	2.24	0.1181	0.1185	2.27	0.1148	0.1149
30 $\bar{3}$ 0	2.13	0.1310	0.1311	2.15	0.1279	0.1280
21 $\bar{3}$ 1	1.84	0.1759	0.1758	1.86	0.1716	0.1719
1340	1.77	0.1897	0.1894	1.79	0.1848	0.1849
30 $\bar{3}$ 1	1.70	0.2054	0.2059	1.72	0.2002	0.2004
2241	1.54	0.2497	0.2496	1.56	0.2434	0.2431
32 $\bar{5}$ 0	1.46	0.2774	0.2768	1.48	0.2703	0.2703
0002	1.41	0.3001	0.2994	1.43	0.2893	0.2894
32 $\bar{5}$ 1	1.30	0.3513	0.3517	1.32	0.3431	0.3427

* relative intensities are indicated in table VII.

intensity would occur. This means that even at the extreme degree of substitution considered in the first possibility the 01 $\bar{1}$ 2, 21 $\bar{3}$ 1, and 12 $\bar{3}$ 2 reflections would certainly be detected whereas in the second, and more unlikely, the 21 $\bar{3}$ 1 reflection would easily be seen. In the light of these conclusions the powder data were re-indexed on a smaller hexagonal unit cell (Table IX).

Discussion

The importance of the charge to radius ratio of the cations in determining the structural type assumed by crystals has long been

recognized. More recently it has emerged that many of the properties of melts can be discussed in terms of cation influence. The term field strength was introduced by Dietzel¹ to define the coulombic attraction of cations at the centre of anion groups. Here Z/a^2 (Z = cation charge, a = cation-anion distance) values are used to express a relative measure of the ability of cations to compete for their coordination requirements.

The work of Bockris² and his co-authors consolidated earlier views that silicate melts are ionic in character. It was a general conclusion from their work that complex silicate anions exist in silicate melts and that their nature and size are influenced by the concentration and field strength of the cations.

The high field strength of the Be^{2+} ion influences the manner in which it distributes itself in crystalline structures. In minerals where beryllium ions predominate the anion units in the structures are small, e.g. O^{2-} , SiO_4^{4-} , $\text{Si}_2\text{O}_7^{6-}$, BO_3^{3-} , PO_4^{3-} . It can be argued that this is a consequence of the strong interaction energy between Be^{2+} ion and near-neighbour oxygen ions which prevents a stable extension of Si-O linkages to form larger anions. It is to be noted, for example, that a beryllium metasilicate has never been characterized.

The association of beryllium with cyclosilicate minerals is a feature of note. Epididymite, $\text{NaBeSi}_3\text{O}_7(\text{OH})$, has been shown³ to be constructed of Si_6O_{15} rings held in double sheets by BeO_4 tetrahedra. A unique fused ring unit, $\text{Si}_{12}\text{O}_{30}^{12-}$, occurs in milarite⁴, $\text{KBe}_2\text{AlCa}_2\text{Si}_{12}\text{O}_{30}$. Significant quantities of beryllium occur in tourmaline, $\text{NaMgB}_3\text{Si}_6\text{O}_{27}(\text{OH})_4$, one of the rare minerals containing $\text{Si}_6\text{O}_{18}^{12-}$ rings, which may be regarded as discrete anionic radicals;⁵ in this structure the ring does not have the equatorial plane of symmetry, which appears to be unique to beryl. In beryl, the rings are symmetrically surrounded by Be^{2+} ions in fourfold co-ordination and Al^{3+} in sixfold co-ordination.⁶

¹ A. Dietzel, *Zeitschr. Elektrochem.*, 1942, vol. 48, p. 9.

² J. O'M. Bockris, J. D. Mackenzie, and J. A. Kitchener, *Trans. Faraday Soc.*, 1955, vol. 51, p. 1734; J. O'M. Bockris, J. A. Kitchener, and S. Ignatowicz, and J. W. Tomlinson, *ibid.*, 1952, vol. 48, p. 75; J. O'M. Bockris, J. A. Kitchener, and A. E. Davis, *ibid.*, p. 536; J. W. Tomlinson, M. S. R. Haynes, and J. O'M. Bockris, *ibid.*, 1958, vol. 54, p. 1822.

³ Е. А. Победимская и Н. В. Белов [E. A. Pobedimskaya and N. V. Belov], Докл. Акад. наук СССР (*Compt. rend. Acad. Sci. URSS*), 1959, vol. 129, p. 900.

⁴ Н. В. Белов и Т. Н. Тархова [N. V. Belov and T. N. Tarkhova], *ibid.*, 1949, vol. 69, p. 365; [Н. В. Белов] N. V. Belov, *Journ. struktur. chem. (USSR)* (translation of *Журн. структур. хим.*), 1960, vol. 1, p. 35.

⁵ G. E. Hamburger and M. J. Buerger, *Amer. Min.*, 1948, vol. 33, p. 532.

⁶ W. L. Bragg, *The Structure of the Silicates*, Leipzig, 1932.

The high temperature reactions exhibited by beryl and its melt can be referred to the possible modes of breakdown that the rings undergo with due regard to the cation influence. Consider the disintegration of a complex silicate anion $\text{Si}_x\text{O}_y^{(2y-4x)-}$. This can be imagined to take place in such a way that a distribution between low-poly- and high-poly-anions results. This has been shown to take place in phosphate melts¹ which, in spite of the difference in basicity between PO_4 and SiO_4 tetrahedra, are in many ways analogous to silicates. It has further been shown² that the proportion of low-polyanion (2 phosphorus atoms/unit) increases with increase in field strength of the cation. Reverting to the silicate anion the extreme type of disproportionation can be represented as: $\text{Si}_x\text{O}_y^{(2y-4x)-} \rightarrow (y-2x)\text{O}^{2-} + x\text{SiO}_2$. It is this type of behaviour that causes immiscibility in melts. Such stratification is well established in silicate melts and again can be related³ to the difference in field strength between the cation concerned and Si^{4+} . It is in the light of this competitive aspect of cation-oxygen association, resolved in some instances by phase separation, that many of the observations made on beryl melts and glasses can be interpreted.

All the observations on the phase relationships recorded in the beryl system suggest a microheterogeneous melt which consists of groupings of Be^{2+} , Al^{3+} , SiO_4^{4-} , and O^{2-} ions dispersed in a matrix of the cristobalite type. The thermal breakdown of the beryl structure on this basis may be formally expressed as $\text{Si}_6\text{O}_{18}^{12-} \rightarrow n\text{SiO}_2 + (6-n)\text{SiO}_4^{4-} + (2n-6)\text{O}^{2-}$ where n may be 3, 4, 5, or 6, according to temperature and possibly the cations.

No evidence was found of other anionic species on the basis of phase generation and it appears that the combined concentrations and high field strengths of Be^{2+} and Al^{3+} eliminate units intermediate in size between these small anions and the Si-O-Si network. The degradation of beryl firstly into an orthosilicate+liquid and then into oxide structures before clear melt is attained confirms that n in the above schematic equation increases with the temperature.

The existence of a random cristobalite-type network is supported strongly by the position of the broad diffuse diffraction halo common to all the glasses; by the similarity of the infra-red absorption spectra of beryl glasses and of fused silica, in which a damaged disordered form of

¹ *Modern Aspects of the Vitreous State*, edited by J. D. Mackenzie, London, 1960, vol. 1, p. 63.

² F. D. Richardson, *Chem. and Ind.*, 1961, 29 July, p. 1132.

³ F. P. Glasser, I. Warshaw, and R. Roy. *Phys. and Chem. of Glasses*, 1960, vol. 1, p. 39.

crystalite linkage is the accepted model; by the lack of a heat effect when α (low)-crystalite crystallizes; and by the ready devitrification of this last phase under a wide variety of thermal treatments.

Strong presumptive evidence for the microheterogeneous distribution of Be^{2+} , Al^{3+} , SiO_4^{4-} , and O^{2-} ions in this matrix is provided by the pattern of non-equilibrium crystallization paths followed as a function of the rate of temperature change. The field strengths of Be^{2+} and Al^{3+} ions are very similar and hence their interaction energies with O^{2-} and SiO_4^{4-} anions in the melt at high temperatures are likely to be similar. On rapid cooling ($> 750^\circ \text{C}/\text{sec}$) to below approximately 1000°C the random distribution of the small ions in the cristobalite matrix is retained and glass transformation results. Slower cooling ($< 250^\circ \text{C}/\text{sec}$) allows diffusive rearrangement and BeO and mullite precipitate metastably at a pseudo-eutectic temperature that varies between 1320° and 1380°C according to the cooling rate. At intermediate cooling rates (350° – $750^\circ \text{C}/\text{sec}$) the undifferentiated association of Be^{2+} , Al^{3+} , SiO_4^{4-} , and O^{2-} ions is preserved in the hybrid structure. The transition process between the formation of this phase and that of BeO and mullite is clearly depicted during thermal analysis at $350^\circ \text{C}/\text{sec}$. The hybrid is metastable and decays readily into phenakite and chrysoberyl, the same products into which BeO and mullite also transform, albeit more leisurely.

The X-ray-powder spectrum of the hybrid bears a strong resemblance to that of phenakite. The unit-cell dimensions, however, imply a closer-packed structure, the c -axis translation being almost identical to that of mullite.

Mullite is now considered to be an orthosilicate in which chains of octahedrally co-ordinated Al^{3+} ions are bound together by tetrahedra randomly filled with Si^{4+} and Al^{3+} ions. Statistical deficiency of oxygen ions occurs according to where the composition lies between the limiting ratios $3\text{Al}_2\text{O}_3 \cdot 2\text{SiO}_2$ and $2\text{Al}_2\text{O}_3 \cdot \text{SiO}_2$. The ionic ratios in the lattice of mullite of composition $2\text{Al}_2\text{O}_3 \cdot \text{SiO}_2$ are SiO_4^{4-} , 4O^{2-} , and 4Al^{3+} . The introduction of 3Be^{2+} in place of 2Al^{3+} would preserve charge balance to give a new ionic ratio of SiO_4^{4-} , 4O^{2-} , 2Al^{3+} , 3Be^{2+} . This is exactly the composition that would arise in the small-ion phase of beryl melts if disproportionation were complete according to



Further, this ionic ratio is exact for the formation of the daughter products chrysoberyl and phenakite.

On these arguments and from the experimental evidence the hybrid can be regarded as a beryllium-containing mullite. That phenakite is the other end-member structure is also strongly suggested by the X-ray evidence. Since phenakite and mullite have different symmetries, only a limited ratio of Be:Al is likely to be tolerated in such a hybrid. The small but definite cell-size variation of the phase when generated from melts with differing Be:Al ratios is thus explained. That the hybrid is a beryllium-containing mullite is also consistent with enlargement of

TABLE X. Calculated lattice energies

Compound	Mol. energy (kcal)	
	on 24-oxygen cell basis	
	a*	b†
BeO	27 380	25 750
BeAl ₂ O ₄	28 690	28 760
3Al ₂ O ₃ , 2SiO ₂ (mullite)	31 640	31 700
Be ₂ SiO ₄	32 350	31 450
SiO ₂	37 320	36 960
Be ₃ Al ₂ Si ₅ O ₁₈ (beryl)	34 300	34 900
Mg ₂ Al ₃ Si ₅ AlO ₁₈ (cordierite)	32 860	33 000

a* Calculated according to the method of M. L. Huggins and K. H. Sun, Journ. Phys. Chem., 1946, vol. 50, p. 319.

b† Calculated according to the method of A. F. Kapustinskii, Quart. Rev., 1956, vol. 10, no. 3, p. 283.

the cell size that occurs when the smaller cell structure is thermally decomposed. The implication here is that Be²⁺ ions diffuse out of the structure more quickly than the Al³⁺ ions, which are temporarily enriched.

The calculated lattice energies of the phases involved are consistent with many of the phase relationships observed (table X). It is not uncommon for simpler structures that require less energy of formation to crystallize from melts before the thermodynamically stable phase. It can be seen that the energies increase through the sequence BeO, BeAl₂O₄, mullite, phenakite, and SiO₂. This represents the order of phase generation during the slow cooling of beryl melts. Further, on this basis, chrysoberyl and phenakite would be expected to be preferred to BeO and mullite since the sum of the lattice energies of the former pair is greater.

Analogous arguments to those used to explain the crystallization

sequences in beryl melts can be used to explain the devitrification processes observed in the glass. If the glass is considered to contain the same elements of short-range order as existed in the melt, the rate of supply of thermal energy would then be expected to control the primary ordering processes in a sequence corresponding to that occurring in melts chilled at differing rates. This expected symmetry of phase generation occurs. Shock-heating produces the hybrid phase whereas glasses leisurely heated (d.t.a.) or glasses thermally conditioned just below the temperature at which any devitrification occurs (850° C) precipitate BeO and mullite.

The reluctance of beryl to grow at any temperature from a melt or glass of its own composition must be related to large energy barriers to the interaction between the open framework of cristobalite and the closer-packed orthosilicates and oxides. Three types of strong bond, Si-O (106 kcal/mol); Al-O (79 kcal/mol) and Be-O (63 kcal/mol) must break before reconstruction can occur.

It is not clear, however, why beryl does eventually reconstitute from the other beryllium aluminium metasilicate glasses. It is to be noted that in their recent communication describing beryl growth by flame-fusion methods, Gentile, Cripe, and Andres (*loc. cit.*) state that compositional changes occur during the process. These may be such as to place the true ratio of reacting oxides into an area of the diagram where beryl is the primary phase. Phase studies over a wide area of the ternary diagram are required before these anomalies can be clarified. It is of interest to note here that these anomalies do not arise in the case of cordierite ($Mg_2Al_3Si_5AlO_{18}$), which is isostructural with beryl. Cordierite readily grows from a glass of its own composition and reassembles below the peritectic point (also at 1450° C) at which it forms mullite + liquid. The much reduced bond energy of Mg-O (37 kcal/mol) not only implies lower energy barriers to rearrangements but results in cordierite having a lower lattice energy. The point has been made above that the calculated lattice energy can frequently be related to the ease of formation from melts but more valid energy data on silicate compounds needs to be accumulated before the conditions of coexistence and mutual transformation of phases in many industrially important systems can be predicted.

Acknowledgement. This paper is published with the permission of the Director of the National Chemical Laboratory.

[Manuscript received 26 March 1964]
